Effects of external stress on defect complexes in semiconductors

2007 J. Phys.: Condens. Matter 19 266201

(http://iopscience.iop.org/0953-8984/19/26/266201)

IOP PUBLISHING JOURNAL OF PHYSICS: CONDENSED MATTER

J. Phys.: Condens. Matter **19** (2007) 266201 (10pp) doi:10.1088/0953-8984/19/26/266201

Effects of external stress on defect complexes in semiconductors

Genene Tessema

Department of Physics, Addis Ababa University, PO Box 1176, Addis Ababa, Ethiopia
and
Helmholtz-Institut für Strahlen und Kernphysik, Nussalle 14-16, 53115 Bonn, Germany

E-mail: genene@gmx.net

Received 21 March 2007, in final form 17 May 2007
Published 4 June 2007
Online at stacks.iop.org/JPhysCM/19/266201

Abstract

Crystal field gradients that exist at lattice sites in solids depend on the symmetry of charge distribution around atomic sites. The charge symmetry could be broken either by the presence of impurity complexes in the host matrix or by external stress on the samples, which leads to an observable magnitude of electric field gradients (EFGs). The perturbed γ–γ angular correlation (PAC) method is employed here to investigate the effect of uniaxial stress on ^{111}Cd sites in crystalline doped semiconductors.

1. Introduction

Atomic lattice sites in solids experience electromagnetic (EM) fields which are produced by the surrounding charges. The fields are mainly caused by charges of the atoms themselves and/or the nearby atoms or molecules. These fields are very large, especially at the nuclear sites. The interaction of such electromagnetic fields with nuclear moments led to the inventions of several nuclear spectroscopic techniques, which are indispensable methods for investigation of the local microscopic environments of atoms in matter. The PAC is one of the techniques that utilizes the interaction between the nuclear moments and the extranuclear fields. The distribution of charges at probe sites, in the diamond type lattice, possesses a cubic symmetry, resulting in zero net field gradient. However, the symmetry can be broken either by the involvement of impurity atoms next to the probe site or by the action of external applied forces. We discuss here the electrostatic field gradient produced by an asymmetric charge distribution of atoms in the diamond lattice structures. The donor–acceptor impurity pairs are the most common types of defect complexes in silicon and germanium that produce a net electric field gradient on the lattice sites. Several of the substitutional and interstitial impurity complexes have been detected by employing the perturbed γ–γ angular correlation method [1, 2].

The theoretical understanding of a crystal field gradient is often very controversial because of the complex nature of the charge distribution around the atoms. On the other hand,

experimental techniques such as PAC are only able to measure the fingerprints of the charge distributions. However, despite the complexity of the problem, the theoretical calculations, using the multiple scattering Korringa–Kohn–Rostoker (KKR) Green's function method [3], were able to reproduce the magnitude of the measured EFGs of the indium-donor pairs in semiconductors. This is in fact one step forward in understanding the nature of the EFGs in solid. Moreover, both the experiment and the theory agreed on the high sensitivity of the magnitude of the EFGs for small variations of the lattice parameters [3, 4]. Therefore, in this paper, experimental results of the EFGs produced by external stress as well as trapped impurities will be discussed.

2. Experimental details

Perturbed γ–γ angular correlation (PAC) uses an unstable radioactive probe nucleus as a tool to investigate the microscopic environments of atoms in the host matrix. The indium isotope (^{111}In) is used as a probe for all measurements here, and decays to ^{111}Cd via electron capture (EC) processes. The intermediate state of the γ–γ cascade that follows the EC decay has a half-life of $t_{1/2} = 84$ ns. This time window enables the observation of the interaction between the moments of the intermediate state of ^{111}Cd and the extranuclear fields. Details of the PAC method can be obtained from the literature and text books [5–7].

The coincidence time spectra $N(\theta, t)$ are measured by the fast–slow pulse processing technique using a setup of four BaF_2 detectors. From the measured spectra, the time differential anisotropy was calculated by the relation $R(t) = 2 \cdot [N(180°, t) - N(90°, t)]/N(180°, t) + 2N(90°, t)$. The parameters of the interactions can be deduced from the ratio function $R(t)$ by comparison with the theoretical perturbation function $G_{22}(t)$,

$$R(t) = A_{22} \sum_i f_i G^i_{22}(t) \tag{1}$$

where A_{22} is the anisotropy coefficient and f_i is the fractions of the probe nuclei at a unique environment i. For a given type of interaction, the time-dependent perturbation function can be written as

$$G^i_{22}(t) = \sum_{n=0}^{3} S^i_n \cos(g_n(\eta)\omega^i_0 \cdot t) \exp[-g_n(\eta)\omega^i_0 \delta^i \cdot t]. \tag{2}$$

The fundamental precession frequency (ω_0) is given by the relation $\omega_0 = (3/10)\nu_Q$. Thus, the quadrupole coupling constant is written as $\nu_Q = eQV_{zz}/h$, where Q and V_{zz} are the quadrupole moment and the principal component of the EFG tensor, respectively.

The applied stress is created by pressing the sample between two cylinder heads, as depicted in figure 1. Here we employed a very shallow implantation depth, about 80 nm beneath the surface, so that the stress near the surface is considered to be uniaxial. For small linear deformation the stress σ can be written as

$$\sigma \propto E \cdot \frac{\Delta L}{L} \tag{3}$$

where E is the elastic modulus, which depends on the nature and the crystal axis of the sample. Based on the change in optical geometry of the reflected laser beam from the curved surface, it is possible to measure the relative change in the sample's length as $\frac{\Delta L}{L} = \frac{D}{2R+D}$ [4], where D and R are the thickness and radius of curvature of the sample.

Samples were prepared from Czochralski (CZ) grown germanium and silicon crystal wafers with surfaces $\langle 100 \rangle$ and $\langle 110 \rangle$, respectively. They were cut to a size of 7×20 mm^2 and doped with different impurities by implantation. The lengths of the samples were intentionally

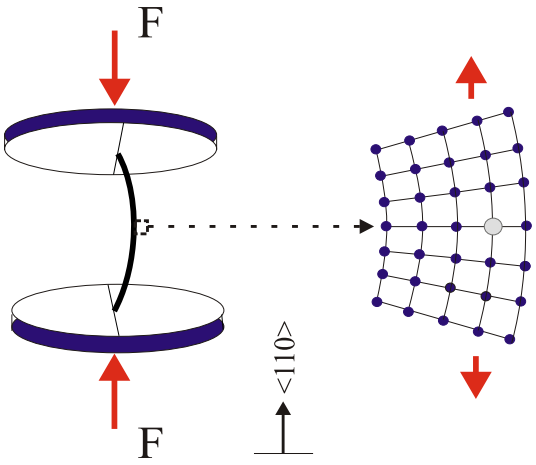

Figure 1. Applied uniaxial stress on crystal samples. The dark circles denote the host atoms, while the shaded circle is the position of the probe atom.

(This figure is in colour only in the electronic version)

Table 1. Implantation parameters.

	Implantation dose (atoms cm^{-2})		
Impurity	Energy	Germanium	Silicon
^{111}In	160 keV	10^{12}–10^{13}	Same
^{75}As	120 keV	1×10^{15}	4×10^{12}
^{115}In	120 keV	—	5×10^{14}

cut along the ⟨110⟩ crystal axis to be able to transmit the applied stress along the same axis. Table 1 contains all the implantation parameters used in the preparation of the samples. The purpose of the incorporation of ^{115}In in silicon will be discussed in section 3.2. The donor–acceptor implantation profiles were deliberately chosen to overlap each other in order to increase the interaction probability of the ionized impurities. Subsequently, the PAC time spectra were taken at room temperature, with and without stress, after annealing the samples in a 10 min isochronal annealing program in vacuum ($\sim 8 \times 10^{-6}$ mbar).

3. Results and discussion

3.1. Formation and properties of the acceptor–donor complexes in semiconductors

Impurity complexes in semiconductors are caused by the presence of either residual or intentionally doped impurities. The foreign atoms preferably occupy various lattice sites in the host matrix, which determines their positive or/and negative contribution as a dopant. The In–As pair in germanium, which is discussed here, is representative of the formation and properties of most intentionally doped substitutional impurity complexes in silicon and germanium [8–16].

The time spectra taken right after the implantation of As and ^{111}In in germanium showed severely damaged lattice environments of the probe atoms. The anisotropy drops to the minimum value expected for static quadrupole interaction. Figure 2 showed the PAC time

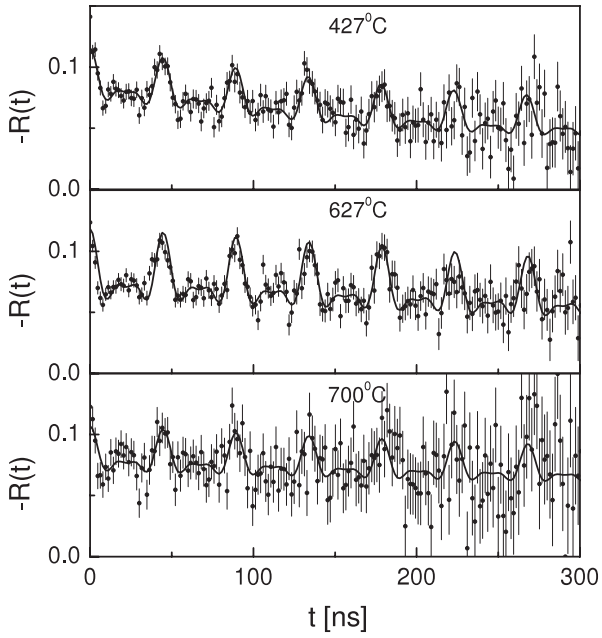

Figure 2. PAC time spectra of the In–As complex in germanium. The solid lines are least-squares fits to the data according to equation (1).

spectra taken recently from an arsenic-doped germanium sample. The first panel of figure 2 is the spectrum taken after annealing the sample at 427 °C in vacuum. A quadrupole interaction frequency of $\nu_Q = 148(1)$ MHz and $\eta = 0$ were derived from the least-squares fits to the data according to equation (1). This frequency was assigned to the In–As complex in germanium [2]. The population of the complex varies with annealing temperature, as is clearly seen by the change in amplitudes in the measured time spectra (see figure 2). The spectrum in the first panel showed that 26(2)% of the probe atoms in the sample have been decorated with arsenic atoms, i.e. each substitutional probe atom in the ensemble is paired with a single arsenic atom as its nearest neighbour (site 1). The population of the same complex grew to 35(2)% of the probe atoms after annealing the sample at 627 °C. However, it is then dropped to 18(2)% at 700 °C. Such a rapid change in population of the complex in a relatively small temperature interval suggests that the binding energy of the In–As complex in germanium is weaker than in silicon. Based on the first-order kinematics, the dissociation energy of the $InAs_1$ in germanium is determined to be 3.27(4) eV less than that of the same complex in silicon which amounts to 3.54 eV [1]. Furthermore, the host matrix also plays a significant role in the magnitude of the EFGs produced by impurity complexes. For instance, the quadrupole coupling constant of the $InAs_1$ in silicon surpasses by 64% the same complex in germanium. This in fact indicates that the disturbances produced by an arsenic atom next to the probe sites in germanium are much weaker than in silicon. Besides, the preliminary tests of the effects of external stress on doped germanium samples showed no indication of the influence of the stress at the various sites in the substrate lattice. Germanium, which is brittle in nature, can hardly change the charge symmetry at the probe sites by varying the lattice constants by about 0.1% in the doped state, unlike silicon, which will be discussed in the following sections.

The quadrupole interaction frequencies of some substitutional group III–V complexes, in crystalline germanium and silicon, are given in figure 3 according to the donors nuclear sizes.

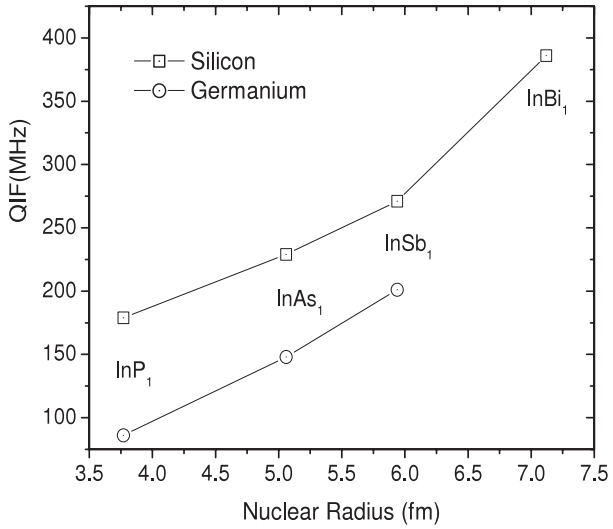

Figure 3. The dependence of the EFGs on the nuclear radius of the donor atoms paired with the probe (^{111}In) in crystalline silicon and germanium. The lines are guides to the eye.

The figure shows not only the increasing trend of the QIF with nuclear radius but also carries information on the dependence of the QIF on the host matrix. The interaction frequency of the same impurity complex varies on an average by ∼81 MHz between silicon and germanium substrates. This difference is mainly associated with the longer tetrahedral covalent radius of the germanium atom, which kept impurities at a distance from its environs compared to that of silicon. However, this frequency margin becomes lower as the impurity nuclear radii increase, which enhances the internal strain in the host lattice.

The field gradient at the nuclear site can be written as

$$V_{zz} \simeq (1 - \gamma_\infty) V_{zz}^{\mathrm{Ext}} + (1 - R) V_{zz}^{\mathrm{Loc}} \tag{4}$$

where the first term arises from electrons and ions outside the nucleus whose fields interact with the probe's nuclear moment. The second term stands for the field produced by unfilled electron shells of the probe atom itself, which is often observed in rare-earth metals. The coefficients are introduced in the equation to include factors that affect the magnitude of the EFGs [17].

3.2. Uniaxial stress on p-type silicon layer

In an effort to understand the effects of applied stress in p-doped crystalline silicon, an indium isotope of ^{115}In was implanted into silicon substrates. This system appeared to be less complicated than n-type silicon due to the electrostatic repulsion between the impurities and the probe atoms. In fact, this experiment is the first of its kind on p-doped silicon. Following the successive implantations of the ^{115}In and the probe (^{111}In) in a silicon sample, respectively, it was annealed at 900 °C in vacuum for 10 min holding time. The implantations were deliberately made in the middle of the samples in order to cause maximum tension on the implanted layer. Moreover, the incorporation of (^{115}In) in the sample was not only intended to create a p-type system but also to check whether the In–In clusters could be formed in silicon. It turned out that no such clusters are detected at the probe sites in the chosen doping level (see table 1). The PAC time spectra are then taken both with and without external stress at room temperature.

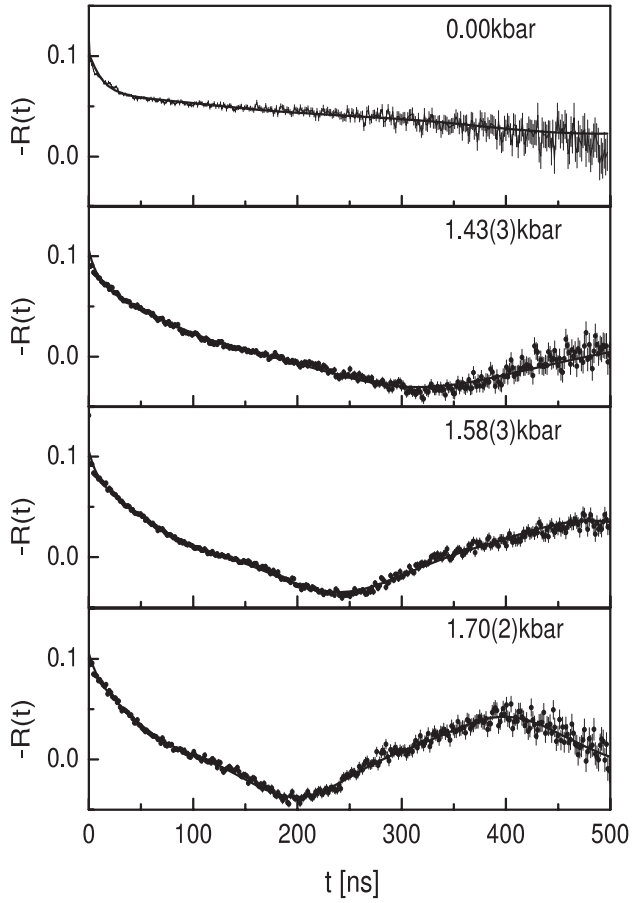

Figure 4. ^{115}In isotope doped silicon layer under uniaxial stress along ⟨110⟩ crystal axis. The solid lines are fits according to equation (1).

Panel 1 of figure 4 is the spectrum taken from the sample without applied stress. This shows that most of the probe atoms possess undisturbed lattice environments, except for the fact that a few of them are located in strained environments caused by pre-implanted oversized indium isotope (^{115}In) in the sample. Thus, almost all substitutional probe atoms possess a symmetric charge distribution in the sample, which is denoted by a flat line on the time spectra (see panel 1 of figure 4). However, the cubic symmetry is broken when the sample is subjected to an external uniaxial stress, resulting in a non-zero crystal field gradient, as observed on panel 2 of figure 4. This spectrum carries an interaction frequency of $\nu_{\mathrm{Q}} = 10(1)$ MHz ($\eta = 0.0$) upon applying 1.43(4) kbar uniaxial tensile stress along the ⟨110⟩ crystal axis. This tension-induced frequency is the result of the net EFG on the probe nuclei due to broken charge symmetry. The frequency generally increases with the value of stress. An interaction frequency of $\nu_{\mathrm{Q}} = 16(1)$ MHz ($\eta = 0.19(1)$) was determined at 1.70(2) kbar. Other hyperfine interaction parameters such as the asymmetry (η) begin to vary slightly above 1.43(4) kbar (table 2). This is indeed expected from the structural deformation that took place at the probe sites. The flat line in panel 1 of the figure, which stands for the undisturbed substitutional probe sites in the sample, could also suggest the absence of the local field ($V_{zz}^{\mathrm{Loc}} \simeq 0$) which could be produced by an unfilled inner shell of the probe itself.

Table 2. Summary of the results of the effects of uniaxial tensile stress on intrinsic silicon.

Site 0 (undisturbed) stress (kbar)	Uniaxial tensile stress along ⟨110⟩		
	ν_{Q0}	η_0	V_{zz}^{Ext} ($\times 10^{19}$ V m^{-2})
0.00	0.00	0.0	0.0
0.91(4)	3(1)	0.0	15
1.14(3)	5(1)	0.0	25
1.43(4)	10(1)	0.07(2)	49.9
1.58(3)	13(1)	0.18(1)	64.8
1.70(2)	16(1)	0.19(1)	79.8

The stress-induced interaction frequency $\nu_Q = 16(1)$ MHz, as observed in panel 4, corresponds to the EFG $V_{zz}^{Ext} = 79.8 \times 10^{19}$ V m^{-2}, as estimated by equation (4). This field gradient is produced by changing the lattice constants by $\Delta L/L \sim 10^{-3}$ in only one direction.

3.3. Uniaxial stress on n-type silicon

The PAC time spectra were also taken from arsenic-doped silicon samples with a view to studying the effect of external stress on the EFGs produced at the various impurity complexes. Following the implantation of arsenic and probe atoms, the samples were annealed at 800 °C in vacuum for 10 min. This temperature was chosen because of the population of maximum arsenic-related complexes in silicon. It in fact creates favourable conditions for testing the effect of applied stress on different complexes in the sample. The first panel of figure 5 shows the time spectrum, while the sample was free from external stress. It carries two interaction frequencies associated with two different complexes in silicon. The interaction frequencies are $\nu_{Q1} = 229(1)$ MHz ($\eta = 0$) and $\nu_{Q2} = 239(1)$ MHz ($\eta = 0.65$). The first frequency stands for a pair of substitutional arsenic and indium in silicon (site 1), while the second frequency was assigned to two substitutional arsenic clusters around a probe atom (site 2) [14]. The fractional population of the In–As$_x$ pairs was extremely high compared to other donor species reported in crystalline silicon. This is presumably due to the similar tetrahedral covalent radii of arsenic and the host atom silicon. After annealing the sample at 800 °C, the population of the InAs$_1$ pair (site 1) was found to be $f_1 = 44(2)\%$ of the probe atom in the sample, while the InAs$_2$ (site 2) accounts for only $f_2 = 25(2)\%$. The undisturbed substitutional probe atoms in the same sample are determined to be $f_0 = 23(2)\%$. The rest of the probe atoms not mentioned here are situated in undefined locations. When the sample is subjected to an external uniaxial compressional stress, the entire spectrum has been modulated by a slowly varying frequency (panel 2 of figure 5).

A frequency of 8(1) MHz was detected at an external stress of 1.22(4) kbar. The newly detected low frequency is the result of the distortion of the cubic symmetry of the indium environment (site 0) by the applied stress. The amplitude of modulation of this frequency is very low because of the small population of site 0 in the sample. This tension-induced frequency (ν_{Q0}) varies approximately linearly with applied uniaxial stress (see figure 6). A maximum value of 23(1) MHz is attained at 2.01(5) kbar in this sample. The interaction frequencies of the complexes containing ^{111}In and As remain unchanged for all possible values of stress (see figure 6). If there is any effect at all on the InAs$_x$ complexes, it is well within the error bars and could not be verified by this method. The only effect observed from these sites was the slight variation in the asymmetry parameter (by $\eta \simeq 0.06(3)$) on the InAs$_1$ complex (see table 3). The absence of detectable changes in the QIF of the InAs$_x$ suggests that no

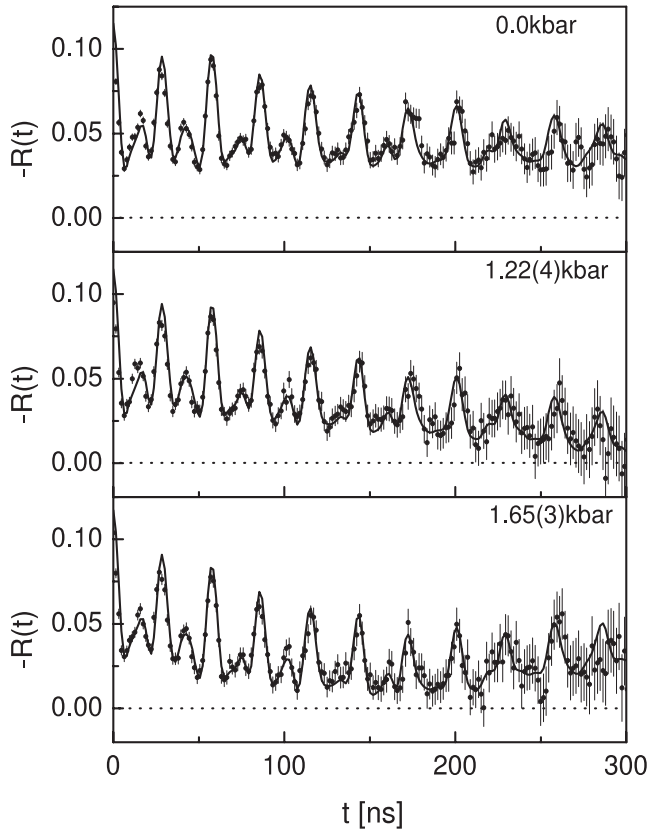

Figure 5. n-doped silicon under the influence of uniaxial stress along the ⟨110⟩ crystal axis. The solid lines are least-squares fits according to equation (1).

(very small) lattice relaxation takes place at these sites. This could probably be due to the high strain field around the complexes, which might prevent further lattice relaxation at the probe sites by external stress. Furthermore, if we look at other hyperfine parameters of site 0 in the sample, the values of the frequency damping are relatively high ($\delta_0 \simeq 25\%$) which indicates a large width of the frequency distribution around the mean value. Such a large width of the frequency distribution is often attributed to the nonuniform probe environments in the implanted layer and the small population of site 0.

3.4. Conclusion

The crystal field gradients have been studied in semiconductors, which happen to be created by external uniaxial stress and by the involvement of impurities next to the probe atoms. The external stress produces a detectable magnitude of EFGs on undisturbed sites (site 0) of the probe atoms situated in the samples. However, the QIF of all the $InAs_x$ complexes in n-doped samples could not vary with applied stress beyond the error margin. This might be due to the high strain field around the complexes created by the presence of oversized impurities in the host lattice. The stress-induced interaction frequencies from undisturbed sites are found to be directly proportional to the magnitude of the stress. Finally, the EFGs produced by impurities

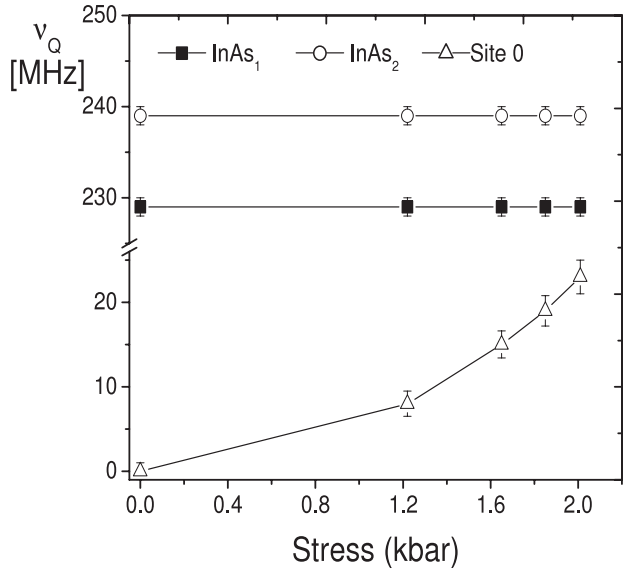

Figure 6. The result of the action of uniaxial stress on the various complexes in an arsenic-doped silicon sample. Tension-induced frequencies could only be observed from a donor-free substitutional fraction (site 0). The $InAs_x$ complexes remain unchanged for all possible values of stress.

Table 3. Summary of the results of the In–As_x pairs under uniaxial stress along the ⟨110⟩ crystal axis in silicon.

Impurity complexes	Uniaxial stress along ⟨110⟩				
	0.0 kbar	1.22(4) kbar	1.65(3) kbar	1.85(3) kbar	2.01(5) kbar
ν_{Q1} ($InAs_1$) (MHz) (site 1)	229(1)	229(1)	229(1)	229(1)	229(1)
η_1	0.0	0.01(2)	0.03(1)	0.06(3)	0.05(2)
δ_1 (%)	0.85(6)	0.82(6)	0.80(6)	0.80(6)	0.55(6)
f_1 (%)	44(2)	44(2)	44(2)	44(2)	44(2)
ν_{Q2} ($InAs_2$) (MHz) (site 2)	239(1)	239(1)	239(1)	239(1)	239(1)
η_2	0.65	0.65	0.65	0.65	0.65
δ_2 (%)	0.95(6)	0.95(6)	0.95(6)	0.95(6)	0.95(6)
f_2 (%)	25(2)	25(2)	25(2)	25(2)	25(2)
ν_{Q0} (undisturbed) (MHz) (site 0)	0.0	8(1.5)	15(1.6)	19(1.8)	23(2)
η_0	0.0	0.06(3)	0.31(2)	0.37(5)	0.36(3)
δ_0 (%)	0.0	5(3)	20(4)	21(3)	25(2)
f_0 (%)	23(2)	23(3)	23(2)	23(2)	23(3)

are generally dependent on the sizes and locations of the impurities themselves next to the probe atom, as well as the host matrix.

Acknowledgments

The author is grateful to the German Academic Exchange Service (DAAD) for partially supporting this work. My gratitude goes to Mr Siggi and Dr Eversheim from the Mass-Separator facility of the Helmholtz-Institut für Strahlen-und Kernphysik, Germany, for several

implantations. I thank Dr R Vianden for his constructive suggestions in the preparation of this work.

References

[1] Wichert Th and Swanson M L 1989 *J. Appl. Phys.* **66** 3026
[2] Forkel D, Achtziger N, Baurichter A, Deicher M, Deubler S, Puschmann M, Wolf H and Witthuhn W 1992 *Nucl. Instrum. Methods Phys. Res.* B **63** 217
[3] Settel M, Korhonen T, Papanikkolaous N, Zeller R and Dederichs P H 1999 *Phys. Rev. Lett.* **83** 4369
[4] Marx G and Vianden R 1995 *Phys. Lett.* A **210** 364
[5] Frauenfelder H and Steffen R M 1965 *Alpha–Beta–Gamma-Ray Spectroscopy* vol 2, ed K Siegbahn (Amsterdam: North-Holland) p 997
[6] Schatz G and Weidinger A 1996 *Nuclear Condensed Matter Physics* (New York: Wiley) (translated by J A Gardner)
[7] Wichert Th 1995 *Appl. Phys.* A **61** 207
[8] Tessema G and Vianden R 2003 *J. Phys.: Condens. Matter* **15** 5297
[9] Wichert Th 2001 *Nucl. Phys.* A **693** 327
[10] Deicher M, Keller R, Pfeiffer W, Skudlik H, Steiner D, Rechnagel E and Wichert Th 1989 *Mater. Sci. Eng.* B **4** 25
[11] Deicher M 1992 *Nucl. Instrum. Methods Phys. Res.* B **63** 189
[12] Feuser U, Vianden R, Alves E, da Silva M F, Szilagyi E, Paszti F and Soares J C 1991 *Nucl. Instrum. Methods Phys. Res.* B **59/60** 1049
[13] Swanson M L, Wichert Th and Quenneville A F 1986 *Appl. Phys. Lett.* **49** 265
[14] Wichert Th, Deicher M, Grübel G, Keller R, Schulz N and Skudlik H 1989 *Appl. Phys.* A **48** 59
[15] Tessema G and Vianden R 2005 *Appl. Phys.* A **81** 1471
[16] Keller R, Deicher M, Pfeiffer W, Skudlik H, Steiner D and Wichert Th 1990 *Phys. Rev. Lett.* **65** 2023
[17] Kaufmann E N and Vianden R J 1979 *Rev. Mod. Phys.* **51** 161